Journal of Catalysis **211,** 387–397 (2002)
doi:10.1006/jcat.2002.3738

On the Catalytic Activity of Co_3O_4 in Low-Temperature CO Oxidation

Jonas Jansson,*[,1] Anders E. C. Palmqvist,† Erik Fridell,† Magnus Skoglundh,† Lars Österlund,† Peter Thormählen,† and Vratislav Langer‡

*Department of Chemical Reaction Engineering, Chalmers University of Technology, SE-412 96 Göteborg, Sweden; †Competence Centre for Catalysis, SE-412 96 Göteborg, Sweden; and ‡Department of Environmental Inorganic Chemistry, SE-412 96 Göteborg, Sweden

Received March 13, 2002; revised June 20, 2002; accepted June 27, 2002

Oxidation of CO over Co_3O_4 at ambient temperature was studied with flow reactor experiments, and in-situ spectroscopic and structural methods. The catalyst deactivates during the reaction. The rate of deactivation increased with increasing CO or CO_2 gas-phase concentration but decreased with increased O_2 concentration or increased temperature. Regeneration of the catalyst in 10% O_2/Ar was more efficient than regeneration in Ar alone. The presence of carbonates and surface carbon on the deactivated catalyst was concluded from TPO experiments. None of these species could, however, be correlated with the deactivation of the catalyst. In-situ FTIR showed the presence of surface carbonates, carbonyl, and oxygen species. The change in structure and oxidation state of the catalyst was studied by in-situ XRD, in-situ XANES, XPS, and flow reactor experiments. One possible explanation for the deactivation of the catalyst is a surface reconstruction hindering the redox cycle of the reaction.

Key Words: **cobalt oxide; CO oxidation; in-situ FTIR; in-situ XRD; in-situ XANES; XPS, low-temperature activity; catalyst deactivation.**

INTRODUCTION

Low-temperature active oxidation catalysts are important in many applications. During the cold start of a car CO and hydrocarbons are emitted untreated into the atmosphere. About 80–90% of all emissions from a car are released during the cold start (1–3). Although the length of the cold-start period may be shortened by an improved heat-up of the catalyst (4, 5), the use of low-temperature active oxidation catalysts may further reduce the amount of these emissions. Emissions of CO and VOC in ventilation air from chemical industries, restaurants, and printeries may be reduced by the use of oxidation catalysts. However, the temperature of the exhaust gases are often too low to start the catalytic reaction, in which case low-temperature active catalysts would be preferred (6, 7). In diesel engines the improved fuel economy leads to lower exhaust gas temperatures, which in the future will call for a need to use more efficient low-temperature active catalysts (8). Low-temperature active oxidation catalysts also find applications in recombining dissociated CO_2 in CO_2 lasers used in orbiting applications (9, 10), removal of odor and CO from air at room temperature (11, 12), and in selective CO gas sensors (13, 14).

Cobalt oxide shows very high CO oxidation activity in CO/O_2 mixtures even at ambient temperature (15) and this reaction has been studied by several groups. Yu Yao (16) found that both pure Co_3O_4 and Co_3O_4 supported on alumina had high activity for CO oxidation and obtained kinetic parameters for the reaction. Different CO oxidation activities for Co_3O_4 in terms of light-off temperature, T_{50}, have been reported. Haruta *et al.* (12) found a T_{50} of about 120°C for pure Co_3O_4. Cunningham *et al.* (17) found a T_{50} of −54°C for pure Co_3O_4 and Thormählen *et al.* (15) reported a T_{50} of −63°C for Co_3O_4 supported on Al_2O_3. It was only the preoxidised cobalt oxide catalyst that showed activity at these low temperatures. The activity over a prereduced catalyst or a cobalt oxide without oxidative pretreatment is lower, and for such catalysts T_{50} has been reported to be about 160°C (15, 18, 19, 20). Upon adding Pt or Pd to a Co_3O_4/Al_2O_3 catalyst, Meng *et al.* (20) found that the temperature required for full conversion in CO oxidation could be decreased by 60 K. Mergler *et al.* (21–23) found that a $Pt/CoO_x/SiO_2$ catalyst had an improved CO oxidation activity compared to CoO_x/SiO_2 or Pt/SiO_2. However, Thormählen *et al.* (15) showed that at low temperatures Pt does not promote the CO oxidation over CoO_x/Al_2O_3.

The low-temperature activity of Co_3O_4 is inhibited by the presence of, e.g., water (16, 17), hydrocarbons, and NO (16). Also in the absence of these inhibitors a slow decrease in activity is seen during steady-state CO oxidation at low temperature. Cunningham *et al.* (17) reported a decrease in CO oxidation activity at −54°C after about 100 min of reaction over Co_3O_4. The deactivation was suggested to be due to accumulation of carbonates on the catalyst surface. Our group has previously seen that a gradual deactivation

[1] To whom correspondence should be addressed. Fax: +46 31 772 30 35. E-mail: Jonas.Jansson@volvo.com.

0021-9517/02 $35.00

takes place during the reaction (24); however, the deactivation could not be correlated with the accumulation of surface carbonates (25). The objective of this study is to further investigate the mechanisms behind the deactivation of Co_3O_4 during CO oxidation at ambient temperature and the regeneration of the catalyst.

EXPERIMENTAL

Materials

The Co_3O_4 catalyst used in all studies was 99.9985% pure Co_3O_4, Puratronic, from Johnson Matthey with a BET area of 4.53 m^2/g.

Flow Reactor Studies

Flow reactor studies were performed in a fixed bed reactor connected to a quadrupole mass spectrometer. The reactor setup has been described in detail elsewhere (24).

The influence of the stoichiometric ratio, $S = 2 \cdot [O_2]/[CO]$, CO concentration, CO_2 concentration, and temperature, T, on the CO oxidation over Co_3O_4 was investigated in a full 2^4 factorial experiment. The levels of the factors are presented in Table 1.

In all reactor experiments the catalyst was first oxidised in 10% O_2 at 550°C for 20 min and cooled in 10% O_2 to the reaction temperature (30°C or 80°C according to the experimental plan). Using mass flow controllers CO, O_2, and CO_2 were then introduced to the reactor during 70 min in the amounts given in Table 1, while the CO conversion continuously was recorded. In these experiments 69.9 mg of catalyst was used, the flow rate was 20 ml (NTP)/min, and Ar was used as balance.

Regeneration of the deactivated Co_3O_4 catalyst was performed by first deactivating the preoxidised catalyst in 1% CO + 0.6% O_2 during 70 min at 22°C and then treating the catalyst for 5 min in either 100% Ar or 10% O_2 at different temperatures (150, 200, 250, 300, 350, 400, 450, 500, or 550°C). After this treatment (regeneration) the activity for CO oxidation was tested at 22°C in a flow of 1% CO + 0.6% O_2. The activity was compared with the activity for the preoxidised catalyst. In these experiments 100.8 mg of catalyst was used, the flow rate was 20 ml (NTP)/min, and Ar was used as balance. The recovery, R, during the regeneration is defined as

$$R = (x_1 - x_d)/(x_0 - x_d)$$

x_1 = CO conversion (%) at 22°C after regeneration

x_d = CO conversion (%) at 22°C after 70 min of deactivation

x_0 = CO conversion (%) at 22°C over the preoxidised catalyst (not deactivated).

The influence of prolonged deactivation was tested by deactivating the Co_3O_4 sample in 1% CO + 0.6% O_2 at 22°C during 70 min and 14 h, respectively. After the deactivation time 10% O_2 was flowed through the reactor, the temperature was raised linearly (10 K/min), and the CO_2 concentration was recorded with a mass spectrometer. In this experiment 100.8 mg of catalyst was used, the flow rate was 20 ml (NTP)/min, and Ar was used as balance.

TABLE 1

Factorial Design for Flow Reactor Study of the CO Oxidation over Co_3O_4

Factor	−	+
S	1.2	3
CO concentration (%)	0.5	1
CO_2 concentration (%)	0	1
Temperature (°C)	30	80

In-Situ FTIR

The in-situ FTIR spectra were recorded by diffuse reflectance using a BioRad FTS 6000. The catalyst powder was placed in a small (6.2-mm diameter × 3.2-mm height) in-situ flow reactor (Harrick Praying Mantis DRIFT cell). The flows of Ar (99.9997% pure), CO, and O_2 (99.998% pure) were controlled by separate mass flow controllers (Bronkhorst High-Tech). The total flow rate was 400 ml (NTP)/min and Ar was used as balance. When the spectra were acquired, 40 scans were averaged to minimise the signal noise. Spectra were recorded in the wavenumber range of 950–8000 cm^{-1} with a resolution of 1 cm^{-1}.

Reference spectra of the catalyst were taken in 100% Ar flow at 20°C after preoxidation in 10% O_2 at 550°C for 90 min and after prereduction in 5% H_2 at 550°C for 30 min. The effect of simultaneous CO + O_2 exposure was studied by introducing 0.3% CO + 0.3% O_2 to preoxidised Co_3O_4 at 20°C. Subsequent FTIR spectra were recorded as a function of time during 85 min (steady-state CO oxidation). The areas of the peaks at 988, 1005, 1044, 1223, 1248, 1270, 1290, 1301, 1321, 1422, and 2164 cm^{-1} were calculated by fitting a partly linear baseline and integrating the spectrum using the method of gaussian deconvolution. In the case of the peak at 2164 cm^{-1}, the contribution from gas-phase CO was identified using the CO rotational lines and then subtracted from the spectra before the area was calculated.

In-Situ XRD

In-situ XRD spectra were obtained with a Siemens D5000 X-ray powder diffractometer using Cu $K\alpha$ radiation ($\lambda = 1.54056$ Å). The Co_3O_4 powder sample was placed in a small corundum (α-Al_2O_3) crucible mounted on a platinum heating plate and positioned inside the in-situ flow reactor cell (AP Paar HTK-10). Reduction of the Co_3O_4

catalyst was studied by flowing 5% H_2 over the fresh sample and increasing the temperature stepwise from 25 to 150, 250, 350, 450, and 550°C. XRD patterns were recorded at each temperature while keeping the temperature constant. Oxidation of the catalyst was studied by first reducing the Co_3O_4 catalyst in 5% H_2 at 550°C, cooling it to 25°C in H_2, and recording the XRD pattern. The gas was then switched to 5% O_2 and the temperature was increased stepwise from 25 to 150, 250, 350, 450, and 550°C. XRD patterns were recorded at each temperature while keeping the temperature constant. CO oxidation was studied by first preoxidising the Co_3O_4 catalyst in 5% O_2 at 550°C and then cooling the catalyst to 25°C and recording the XRD pattern. The gas flow was then switched to 2% CO + 4.9% O_2. XRD patterns were then recorded after 30 min at each of the temperatures 25, 100, and 170°C. In all experiments the total gas flow rate was 500 ml/min and He was used as balance.

In-Situ XANES Analysis

Dispersive Co K-edge XANES measurements were performed in transmission mode at beamline ID24 at ESRF in Grenoble, France, on pressed pellets of powder samples of Co_3O_4. The pellets were mounted in an *in-situ* temperature-controlled flow-through catalytic reactor cell, which was fed with a reactant gas mixture obtained via mass flow controllers. The total flow was 100 ml (NTP)/min. The gas mixture at the reactor outlet was continuously analysed with a Balzers Prisma mass spectrometer. The beamline uses a Si [111] polychromator crystal, operating in Bragg mode, for selection of the desired range of X-ray wavelengths, and a 1152 × 1242 pixel CCD solid-state detector for spectral analysis. Harmonic rejection was achieved through the use of two additional mirrors in the beamline, and the estimated energy resolution was $\Delta E/E \approx 1.2 - 1.5 \times 10^{-4}$. The data analysis was performed using the program Delia in the XAID toolbox of the XOP 2.0 software package (26). The energy scale of the CCD detector was calibrated before and after each measurement series using a Co metal foil and fitting the measured data points to those of a Co foil spectrum taken from the database DABAX in the XOP 2.0 package. The average energy and current in the storage ring during the entire series of measurements was 6 GeV and 180 mA, respectively. XANES spectra were recorded during H_2-TPR in 10% H_2 after preoxidation, O_2-temperature programmed oxidation (TPO) in 10% O_2 after prereduction, temperature programmed CO oxidation in 1% CO + 1% O_2 after either preoxidation or prereduction, and during exposure to 1% O_2 + 1% CO + 10% CO_2 at 50°C for 25 min. Preoxidation was performed at 460°C in 10% O_2 and prereduction at 460°C in 10% H_2. The temperature ramp speed was 20 K/min in all experiments and He was used as balance.

XPS Analysis

XPS analysis was performed using a Perkin Elmer PHI 5000 C system equipped with a pretreatment cell allowing the samples to be exposed to various gas mixtures at 1 atm and transferred between the pretreatment cell and the UHV chamber without being exposed to ambient air. The analysis was performed on a pressed disk of Co_3O_4 after different pretreatments. The sample was initially oxidised in 19% O_2 at 550°C for 20 min, cooled in oxygen, transferred to the UHV chamber and analysed. After this the sample was returned to the pretreatment cell and exposed to either a mixture of 1% O_2 and 0.6% CO or 4% CO at 25°C for 70 min and then analysed again. Finally the sample was reduced in 8% H_2 at 550 °C for 20 min and analysed again. The total flow was 100 ml/min. The XPS spectra were recorded using nonmonochromatic Mg $K\alpha$ radiation. The energy scale was internally calibrated by setting the C1s peak at 284.3 eV.

RESULTS

Influence of O_2, CO, CO_2, and Temperature

The factor experiments for the Co_3O_4 showed that the activity increased and the rate of deactivation was less severe with a higher oxygen concentration. For example, the conversion after 70 min of reaction at 30°C and with a CO concentration of 0.5% increased from 79 to 94% by increasing the oxygen concentration from 0.3% ($S = 1.2$) to 0.75% ($S = 3$). A higher CO concentration (with constant stoichiometric ratio) only influenced the initial activity slightly but the rate of deactivation increased. These results agree with previous findings (24), although in the previous study the CO concentration was kept constant at 2% while in the present work the effect of different CO concentrations was studied. Carbon dioxide present in the reactant gas mixture also increased the rate of deactivation. When the temperature was increased the catalyst showed an increased activity and a slower rate of deactivation. The deactivation of the catalyst could be almost completely avoided by increasing the temperature from 30 to 80°C. The initial conversion of CO to CO_2 and the conversion after 70 min of reaction for all the levels of the parameters are given in Table 2.

Regeneration

The result of the regeneration experiments is presented in Fig. 1. The regeneration does not occur at low temperature (during the reaction) but the catalyst must be heated to 250°C or above. Regeneration in 10% O_2 was more efficient than regeneration in 100% Ar. More than 60% recovery of the initial catalytic activity was obtained after regenerating in 10% O_2 at 250°C while regenerating in 100% Ar less than 30% recovery was obtained even at 350°C (see Fig. 1).

TABLE 2

CO Oxidation over Preoxidised (10% O_2 at 550°C for 20 min) Cobalt Oxide. Effect of Stoichiometric Ratio ($S = 2[O_2]/[CO]$), CO Concentration, CO_2 Concentration, and Reaction Temperature at Steady-State Reaction Conditions

S	CO (%)	CO_2 (%)	T (°C)	Initial conversion (%)	Conversion after 70 min (%)
1.2	0.5	0	30	95	79
3	0.5	0	30	98	94
1.2	1	0	30	93	60
3	1	0	30	98	82
1.2	0.5	1	30	92	59
3	0.5	1	30	99	74
1.2	1	1	30	89	44
3	1	1	30	98	72
1.2	0.5	0	80	99	97
3	0.5	0	80	99	99
1.2	1	0	80	99	96
3	1	0	80	100	98
1.2	0.5	1	80	99	93
3	0.5	1	80	100	97
1.2	1	1	80	99	92
3	1	1	80	100	98

Deactivation during Prolonged Exposure Time

After 14 h of exposure to the reactant gas mixture the catalyst had completely lost its activity. Figure 2 shows the TPO diagrams of the Co_3O_4 after exposure to the 1% CO + 0.6% O_2 during 70 min and 14 h, respectively. In both cases a large CO_2 peak is seen at about 120°C and a smaller peak at about 350°C. Previous analysis of TPO profiles has identified the 120°C peak as carbonates desorbing from the catalyst and the high-temperature peak as oxidation of some sort of surface carbon species (24). The catalyst deactivated for 14 h also showed desorption of CO that started at room temperature. In case (a) in Fig. 2 the TPO started with a high CO_2 concentration since the catalyst still had a high activity and hence a large amount of CO_2 was produced. In case (b) the catalyst had completely lost its activity and no CO_2 was produced. Since no CO_2 had been let into the MS chamber for a long time in the latter case the CO_2 signal had diminished to a low value. The time to reach this low value was longer than 70 min, which was why the CO_2 signal did not reach zero at the end of the TPO experiment in Fig. 2. The area below the graph corresponds to 5.5 respectively 3.9 μmol CO_2 for the sample deactivated during 70 min respectively 14 h. The weight of the sample was 100.8 mg. The total number of surface cobalt atoms can thus be estimated from the BET area (4.53 m^2/g) to 6.8 μmol surface atoms by assuming a number of 9×10^{18} cobalt atoms/m^2 (27) for the Co_3O_4 surface. This means that carbonates and C_{surf} probably cover a large part of the catalyst surface but not the entire surface.

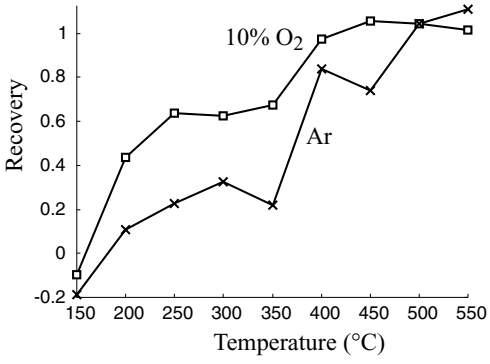

FIG. 1. Effect of regenerating the Co_3O_4 catalyst in 10% O_2 (squares) or 100% Ar (crosses) at different temperatures after the catalyst had been deactivated for 70 min in 1% CO + 0.6% O_2.

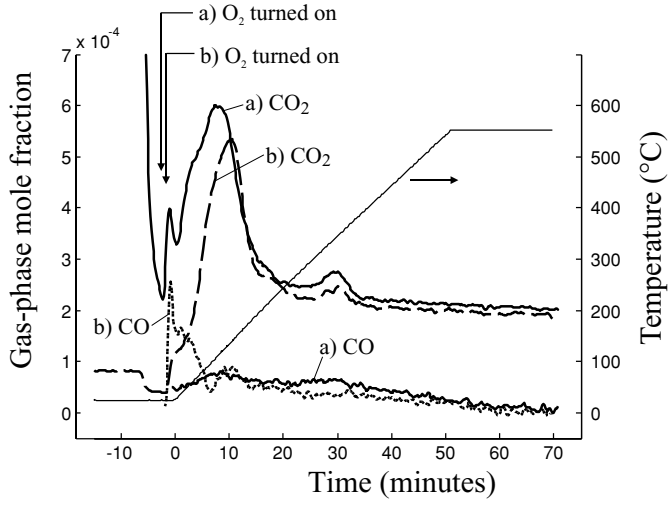

FIG. 2. CO and CO_2 evolution during TPO after deactivation (1% CO + 0.6% O_2) at 22°C during (a) 70 min (solid lines) and (b) 14 h (dashed lines).

In-Situ FTIR

The in-situ FTIR spectrum of preoxidised Co_3O_4 is shown in Fig. 3, spectrum a, where, in order to present the cobalt–oxide specific bands, the prereduced catalyst was used as background when the absorbance was calculated. The preoxidised Co_3O_4 showed strong absorption bands at 988, 1005, 1044 cm^{-1}, and a broad band at 1290 cm^{-1}. The latter consisted of several bands: at 1248, 1270, 1290, and 1301 cm^{-1}. There were also bands at 1146 and 1180 cm^{-1}. Davydov assigned bands in this region to metal–oxygen stretchings of coordinatively unsaturated metal ions and surface oxygen atoms (28). These bands are not present in the reduced catalyst but appear upon preoxidation. The bands at 1248, 1270, 1290, and 1301 cm^{-1} also appear upon preoxidation. However, these frequencies are too high to belong to metal–oxygen stretchings. Carbonates have stretching frequencies in this region, but in this

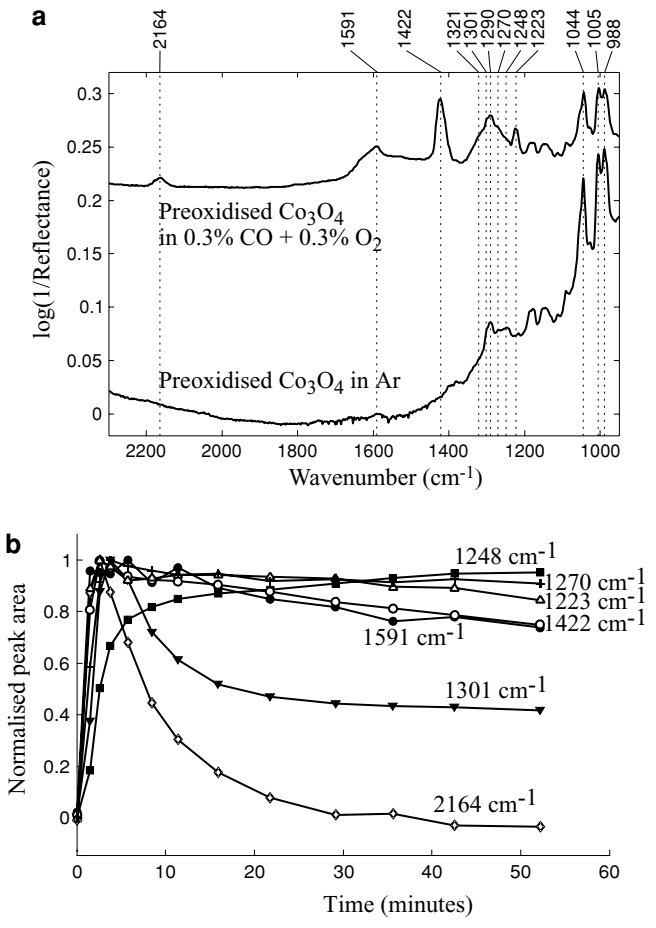

FIG. 3. (a) In-situ FTIR spectra of preoxidised Co_3O_4 in Ar at 20°C (bottom spectrum) and in 0.3% CO + 0.3% O_2 (top spectrum). (b) The evolution of the area of the bands at 1223, 1248, 1270, 1301, 1422, 1591, and 2164 cm^{-1} during the exposure to 0.3% CO + 0.3% O_2 as a function of time.

experiment neither CO nor CO_2 was introduced to the catalyst. Another candidate is an oxide species O_2^{x-}. Charged O_2^{x-} species with x between 0 and 1 have vibration frequencies between 1550 and 1130 cm^{-1} (28). Al-Mashta *et al.* (29) studied O_2 adsorption on preoxidised α-Fe_2O_3 with IR spectroscopy. They found absorption bands at 1270, 1300, 1325, and 1350 cm^{-1}, which were assigned to a perturbed O_2^- species (intermediate between O_2 and O_2^-), and bands at 930, 990, 1010, and 1090 cm^{-1}, which were assigned to perturbed O_2^{2-} (intermediate between O_2^- and O_2^{2-}) or to Fe=O surface bonds.

Figure 3, spectrum b, shows the change in the spectrum when CO and O_2 were introduced to the sample. Here the absorbance was calculated using the spectrum of the preoxidised catalyst as background. The same peaks as those in Fig. 3, spectrum a, were present and in addition new bands at 1223, 1321, 1422, 1591, and 2164 cm^{-1} appeared. The bands at 1223 and 1422 cm^{-1} can be assigned to surface carbonate species (25, 28). We have previously shown that these peaks are doublets consisting of two peaks at 1219 and 1229 cm^{-1}, respectively, two peaks at 1417 and 1432 cm^{-1}. These bands originated from two different surface carbonate species: one that occurred upon CO_2 adsorption and the other after CO exposure. During the reaction between CO and O_2 both of these are present since CO_2 is formed in the reaction. The band at 1591 cm^{-1} is also characteristic of surface carbonates.

The evolution of the bands at 1223, 1248, 1270, 1301, 1422, 1591, and 2164 cm^{-1} during the reaction is shown in Fig. 3. All bands except the band at 1248 cm^{-1} first quite rapidly reached a maximum and then decreased. The decrease in the 1301 and 2164 cm^{-1} bands was faster than the decrease in the 1223, 1422, and 1270 cm^{-1} bands. The band at 2164 cm^{-1} is associated with CO adsorbed to a cobalt ion. Careful inspection of this band (not shown) and the fact that it is quite broad indicates that it consists of two peaks located approximately at 2155 and 2178 cm^{-1}. The frequency of the CO stretch depends on the valency of the cobalt ion. The CO stretch is reported at 2023–2025 cm^{-1} on Co^0, 2070–2110 cm^{-1} on Co^+, 2120–2170 cm^{-1} on Co^{2+}, and 2178–2180 cm^{-1} on Co^{3+} (30–32). The CO stretching frequency can also vary with the exposed cobalt oxide facet, probably because of the different coordination of the cobalt atoms on the different facets affects the orbitals involved in the adsorption of CO to cobalt and thus the CO stretching frequency. For Co^{2+}, Schönnenbeck *et al.* (33) reported a CO stretching frequency of about 2146 cm^{-1} when adsorbed to CoO(100) and 2170 cm^{-1} when adsorbed to CoO(111). The band at 2164 cm^{-1} is thus probably a combination of CO adsorbed on Co^{3+} and Co^{2+} sites or adsorbed on cobalt ions with different coordination.

The split of the 2164 cm^{-1} band in the two bands at 2155 and 2178 cm^{-1} was even more pronounced when CO was adsorbed at 20°C without the presence of oxygen (not shown in the figure). In this case the creation of oxygen vacancies via the formation of CO_2(g) is more pronounced than during the reaction between CO and O_2. As the creation of oxygen vacancies changes the coordination number of the surface cobalt ions the two bands at 2155 and 2178 cm^{-1} probably arise from CO adsorbed on surface cobalt ions with different coordination. The lower frequency species could also arise from CO adsorbed on a cobalt ion that has been reduced to Co^{2+} in the catalytic redox cycle. The decrease in the 2164 cm^{-1} band means that the number of cobalt ion sites available for CO adsorption decreases during the reaction. One possible reason for this could be that the surface reconstructs in a way that cobalt ions available for CO adsorption become less abundant on the surface. Another possibility is that carbonates or OH groups block these sites. Traces of OH stretchings could be detected in the 3300–3700 cm^{-1} region of the FTIR spectra. However, these bands were so weak that it was not

possible to determine whether they increased or decreased during the reaction.

The 1248 cm^{-1} peak increased first rapidly then more slowly during the 85 min of the reaction. It is tempting to assign this band to a surface carbonate accumulating on the surface during the reaction explaining the deactivation of the catalyst. However, this band was also seen on the preoxidised sample when neither CO nor CO_2 were introduced so that no carbonates could have been formed. The preoxidation temperature (550°C for 90 min) should also be sufficient to remove possible contamination of carbonates or carbon containing compounds from the surface. Al-Mashta *et al.* (29) assigned this band to a perturbed superoxide species. The bands at 1270, 1290, and 1301 cm^{-1} are in the same region as the 1248 cm^{-1} band and occurred all upon oxidation of the catalyst without any introduction of CO or CO_2. The bands at 1270 and 1301 cm^{-1} first rapidly increased and then decreased while the band at 1290 cm^{-1} increased during the first 5 min but then remained constant. Following Al-Mashta *et al.* (29) we assign the bands at 1248, 1270, 1290, and 1301 cm^{-1} as originating from the same O_2^{x-} species adsorbed on surface sites of different structures. The increase in the 1248 cm^{-1} band and the decrease in the 1270 and 1301 cm^{-1} bands could then be explained as a redistribution of the type of surface sites where O_2^{x-} is adsorbed, the redistribution being due to the surface reconstruction during the reaction.

The bands at 988, 1005, 1044, 1290, and 1321 cm^{-1} all increased during the first 5 min but then remained constant during the reaction time. The increase of the 988, 1005, and 1044 cm^{-1} peaks means that the amount of surface oxygen atoms bonded to coordinatively unsaturated cobalt ions increased during this time. This might be due to the creation of oxygen vacancies during the reaction. Some of the surface oxygen atoms reacts with CO or CO_2 to form CO_2 or surface carbonates thus creating oxygen vacancies and lowering the coordination number of the surface cobalt ions. The frequencies of the CoO vibration of the remaining oxygen atoms then shifted from the fundamental frequencies (at 571 and 664 cm^{-1} (34)) to the 1000 cm^{-1} region leading to an increase in these peaks.

In-Situ XRD

According to the XRD pattern in Fig. 4 the fresh cobalt oxide sample consisted of pure Co_3O_4. When the sample was heated in 5% H_2 the Co_3O_4 phase remained at 150 and 250°C. At 350°C, however, the peaks for the Co_3O_4 phase decreased and the largest Co peak appeared. Also present at 350°C was one of the peaks for the CoO phase (at $2\theta = 36.3°$). At 450°C the Co_3O_4 and CoO peaks disappeared completely and only the Co phase was visible. At 550°C only Co was present, and even its weaker peak (at $2\theta = 51.1°$) was more pronounced than at 450°C.

Upon treatment in 5% H_2, Co_3O_4 was reduced to Co at a temperature around 350°C. At this temperature CoO

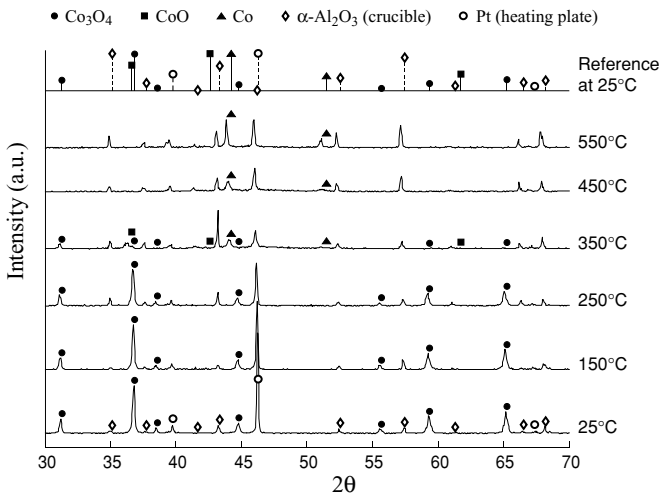

FIG. 4. Reduction of fresh Co_3O_4 in 5% H_2 at different temperatures.

seemed to be formed as an intermediate. The diffractograms were collected by scanning from small θ to large θ. This explains why only the CoO peak at 36.3° is clearly seen, whereas the peak at 42.6° is almost absent, and the peak at 61.7° is not present. Collecting a diffractogram took about 30 min and by the time the angle 42.6° was recorded the CoO phase had almost disappeared.

The in-situ XRD measurements are in agreement with previous TPR and TPO data of cobalt oxide catalysts (24, 35–37). In TPR a main reduction peak was seen at 370°C (24), which agrees with the transition from Co_3O_4 to metallic Co seen at 350°C in the XRD pattern (Fig. 4). XRD also reveals that the reduction takes place via CoO since this phase is present as an intermediate. During the oxidation a transition from Co to Co_3O_4 was seen at 350°C (Fig. 5). This

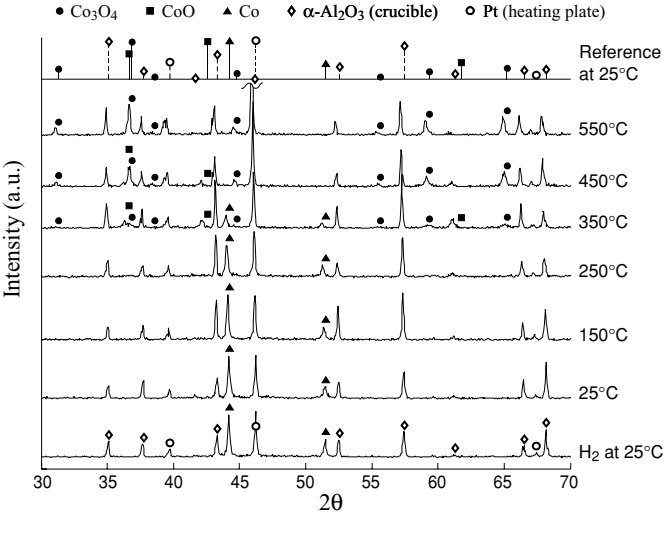

FIG. 5. Oxidation of reduced Co_3O_4 in 5% O_2 at different temperatures. The waved line indicates that the Pt reflection at $2\theta = 46.3°$ has been truncated in the figure.

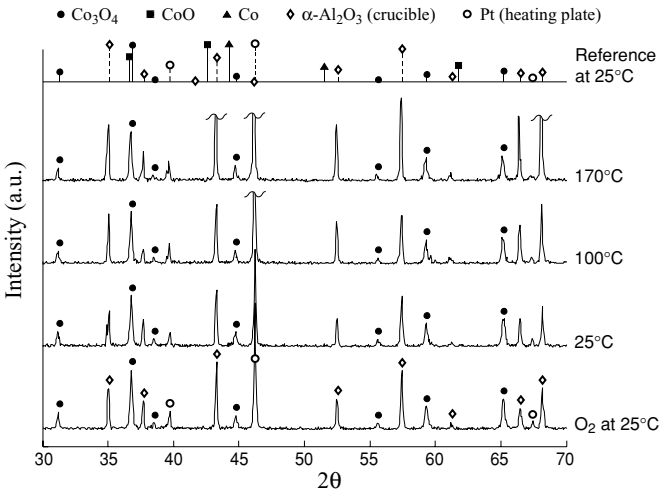

FIG. 6. In-situ XRD during reaction between 2% CO + 4.9% O_2 over preoxidised Co_3O_4. The waved lines indicate that the α-Al_2O_3 reflections at $2\theta = 43.4^\circ$ and 68.2°, and the Pt reflection at $2\theta = 46.3^\circ$ have been truncated in the figure.

agrees fairly well with previous TPO data where a main oxidation peak was present at 245°C with a shoulder at about 350°C.

Exposing the reduced sample for a flow of 5% O_2 at 25°C does not affect the bulk structure of the sample according to the XRD patterns shown in Fig. 5. The sample remained as Co also at 150 and 250°C. At 350°C a decrease in the Co peaks (2θ of 44.0° and 51.2°) was observed, accompanied by the appearance of Co_3O_4 peaks (2θ of 36.7° and 65.1°) and CoO peaks (2θ of 36.3° and 42.2°). This temperature region for formation of Co_3O_4 from the lower oxide agrees well with the temperature region where the catalyst is regenerated (see Fig. 1). Interestingly Co, CoO, and Co_3O_4 seem to coexist at this temperature. Given that lower θ were recorded first; CoO ($2\theta = 36.3^\circ$) and Co_3O_4 ($2\theta = 36.7^\circ$) were detected first, followed by the larger CoO peak at $2\theta = 42.2^\circ$. But after this the Co peaks at 44.0° and 51.2° could be seen so the sample was not yet completely oxidised at this stage. At higher angles still, Co_3O_4 could be seen at $2\theta = 65.1^\circ$ and CoO at 61.7°. At 450°C the Co phase had completely disappeared, and the Co_3O_4 peaks had increased substantially. Some CoO was still present (small peaks at 36.3°, 42.2°, and 61.7°). At 550°C only Co_3O_4 was detected XRD.

For all diffractograms collected at elevated temperature the XRD peaks were shifted to lower 2θ values compared to the references which refer to 25°C. This was caused by the thermal expansion of the crystal lattice.

During the CO oxidation reaction only peaks from the Co_3O_4 phase could be seen at 25°C (Fig. 6). There was no visible difference between the diffractogram of the preoxidised sample in O_2 at 25°C and that of the sample in the reactant gas mixture. Even upon increasing the temperature to 100 and 170°C no visible change in the diffractograms occurred, and the only phase present was Co_3O_4.

From previous isotope labeling experiments (24) the amount of surface Co atoms could be estimated to 3.8% of the total amount of cobalt atoms. Of these surface atoms only a fraction are deactivated (since the catalyst is still quite active). It is thus not probable that this change could be observed with the XRD equipment used, since it measures both surface and bulk Co atoms, and does not detect crystalline phases present in a concentration below 0.25% by volume.

In-Situ XANES

The result of in-situ XANES analysis during H_2-TPR of a preoxidised Co_3O_4 sample is presented in Fig. 7a. The sample remained in an oxidised form up to ca. 425°C, and the transition to metallic cobalt started at about 460°C. After the sample was kept at 460°C for 5 min the sample was completely reduced to metallic cobalt. The result of in-situ XANES analysis during O_2-TPO of

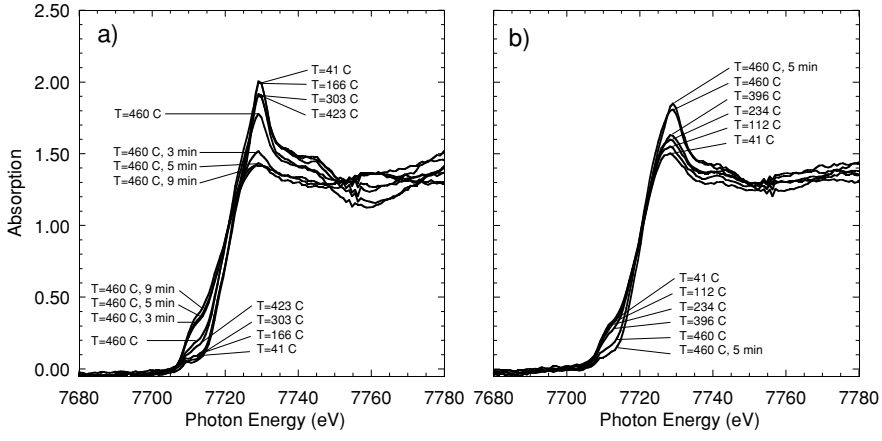

FIG. 7. Co K-edge XANES analysis during (a) H_2-TPR in 10% H_2 of preoxidised Co_3O_4 and (b) O_2-TPO in 10% O_2 of prereduced Co_3O_4.

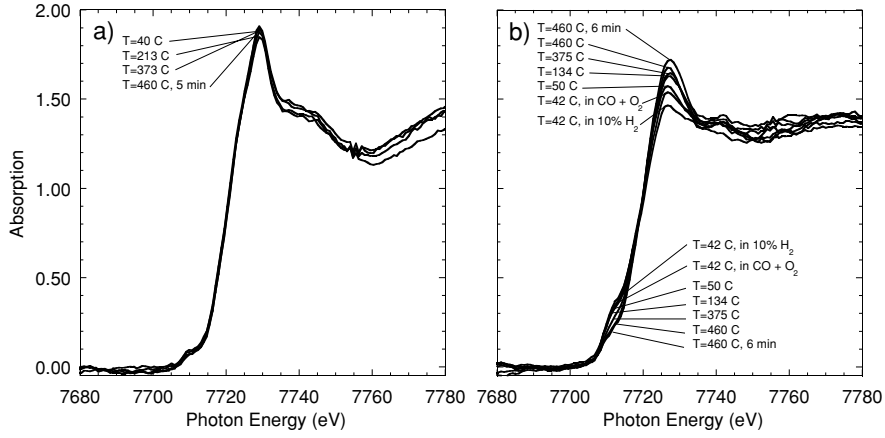

FIG. 8. Co K-edge XANES analysis during CO oxidation in 1% CO + 1% O_2 over (a) preoxidised Co_3O_4 and (b) prereduced Co_3O_4.

a prereduced Co_3O_4 sample is shown in Fig. 7b. After prereduction the sample was in the form of metallic cobalt. A slight oxidation of the sample was seen throughout the temperature range 41–396°C, but the sample was only completely oxidised at 460°C. The reoxidation seemed to go faster than the reduction.

Figure 8a shows the result of CO oxidation over the preoxidised Co_3O_4. During the reaction the catalyst stayed as Co_3O_4 at all temperatures. The preoxidised sample did not show any sign of reduction, which was expected since at 460°C the rate of reoxidation to Co_3O_4 is high. The result of CO oxidation over the prereduced Co_3O_4 is shown in Fig. 8b. The catalyst was initially in the form of metallic cobalt but was gradually oxidised during the reaction. The oxidation started already below 50°C and increased as the temperature was raised. The oxidation was not completed at 460°C but continued as the sample was held there for a period of 6 min. Introduction of CO_2 did not affect the oxidation state of Co_3O_4 during CO oxidation according to XANES, and the catalyst stayed as Co_3O_4.

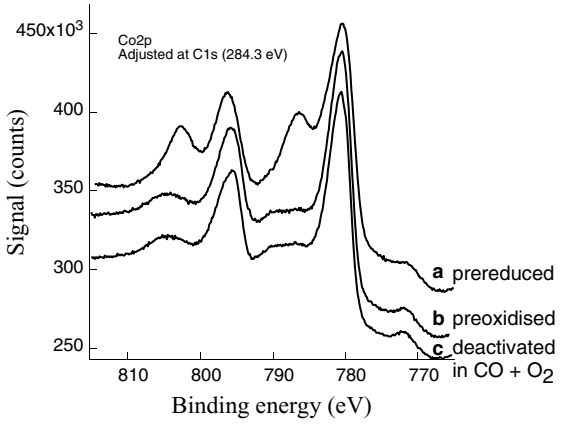

FIG. 9. Co2p XPS spectra (a) after prereduction in H_2 at 550°C, (b) of the preoxidised Co_3O_4, and (c) after 70 min reaction in 1% CO + 0.6% O_2 at 25°C.

XPS Analysis

The resulting Co2p spectra from the XPS analysis are given in Fig. 9. The prereduced sample (a) shows a spectrum that closely resembles what one would expect for pure CoO (38). The spectra for the preoxidised sample (b) and for the sample deactivated in 1% O_2 and 0.6% CO (c), and 4% CO (not shown) at room temperature for 70 min, are very similar. They resemble reference spectra for pure Co_3O_4 (39). Also the O1s spectra are very similar for the three latter pretreatments. No significant accumulation of carbon could be observed after the deactivation pretreatment. Oku and Sato (40) studied cobalt oxide with in-situ XPS and could detect a reversible transition from CoO to Co_3O_4 at 347°C during oxidising conditions. This temperature agrees with the temperature where the oxidation of CoO to Co_3O_4 can be seen with XRD in Fig. 5. Bridge and Lambert (41) observed with LEED that Co_3O_4 grown on Co(0001) was reduced to CoO when exposed to CO and heated to 200°C, and that the CoO could then be oxidised back to Co_3O_4 by exposure to O_2 and annealing at 327°C. However, in our experiments performed at 25°C, no change in oxidation state was observed during the CO oxidation. Not even when the catalyst was severely deactivated by exposing it to 4% CO for 70 min at 25°C could a change in oxidation state of cobalt be detected.

DISCUSSION

The oxidation of CO over Co_3O_4 has been proposed to follow a redox cycle where gas-phase CO adsorbs on a cobalt site, and the adsorbed CO reacts with a lattice oxygen atom forming CO_2(g) and an oxygen vacancy, thus reducing the oxidation state of the cobalt site (24, 25). Reoxidation of the cobalt site then occurs with gas-phase oxygen (24, 25).

In Table 2 it can be seen that the CO conversion over Co_3O_4 was initially high (89–100%) but the catalyst became deactivated with time. The rate of deactivation increased when increasing the gas-phase CO or CO_2 concentration, while increasing the stoichiometric ratio (oxygen concentration) or increasing the temperature decreased the rate of deactivation (Table 2). Several possible mechanisms could explain the observed deactivation of the Co_3O_4 catalyst during low-temperature CO oxidation. Previously, we have proposed the deactivation to occur by irreversibly reducing the oxidation state of the surface cobalt ions so that they could not be reoxidised at the low reaction temperature (25). Another possibility is that the active sites are blocked by carbonyl, carbonate, coke, or H_2O/OH species. A third deactivation mechanism could be that the creation of oxygen vacancies when reacting with adsorbed CO leads to a reconstruction of the cobalt oxide surface making the cobalt sites unavailable for CO adsorption.

Several hypotheses can thus be put forward to explain the deactivation of the cobalt oxide catalyst during CO oxidation at ambient temperature. It is often believed that deactivation occurs by blocking the active sites with surface carbonates. In this work, however, it was seen that a temperature of about 400°C was needed to obtain 80% recovery of the activity when regenerating in Ar. This is much higher than what could be expected for desorbing surface carbonates, which is about 100°C (25). With FTIR, the bands originating from surface carbonates at 1223 and 1422 cm^{-1} were seen to decrease during the reaction, opposite to what would be the case if surface carbonates built up on the catalyst and thus deactivated it. A third piece of evidence opposing the carbonate explanation is the TPO after 14 h of deactivation, where the carbonate peak was not larger (but smaller) than the carbonate peak from the catalyst deactivated during only 70 min.

The blocking of active sites by adsorbed CO is not a probable candidate for the deactivation since the bands for CO adsorbed on cobalt sites were seen to decrease with FTIR. If there were a blocking of the sites by CO one would have expected these bands to increase or at least remain constant during the reaction. Adsorbed CO would also probably have desorbed in the regeneration experiment when regenerating in 100% Ar already at about 100°C (15).

It is also possible that carbonaceous species, C_{surf}, might be formed during the reaction, deactivating the catalyst. However, regeneration in oxygen at 250°C was sufficient to regain more than 60% of the activity while the oxidation temperature for C_{surf} is about 450°C (24). If C_{surf} was the major deactivating species a larger high-temperature TPO peak would be expected in the TPO of the catalyst deactivated during 14 h compared to the sample deactivated during 70 min. However this was not seen, and the high-temperature peak is of the same size independent of deactivation time. Further, no significant accumulation of carbon could be observed with XPS after the deactivation pretreatment.

Traces of surface OH groups were detected with in-situ FTIR. This is because traces of water are always present in the gas bottles even when using gases of high purity. It is known that small amounts of water deactivate the cobalt oxide catalyst (17) and this deactivation probably occurs by H_2O_{ads} or OH groups blocking the active cobalt ions. However, this hypothesis cannot explain why the catalyst was regenerated at a lower temperature when regenerating in 10% O_2 compared to Ar, nor why the deactivation is faster in the presence of a higher CO concentration and lower at higher stoichiometric ratios.

The second mechanism for the deactivation of Co_3O_4 during CO oxidation could be a change in oxidation state of the cobalt in the oxide surface. The observed increased deactivation rate of Co_3O_4 with increasing CO concentration and exposure time agrees with the deactivation model proposed in (25). Increasing the CO concentration would increase the rate of the irreversible reduction of the active cobalt sites leading to a higher rate of deactivation. In this oxygen-vacancy-deactivation mechanism (or slow irreversible reduction mechanism) two types of oxygen vacancies or reduced cobalt sites exist. The first site is an oxygen vacancy created when CO reacts with a lattice oxygen atom and desorbs as CO_2. This oxygen vacancy is readily reoxidised and the reoxidation proceeds at 20°C. The second site is a more reduced site (with lower or partially lower oxidation state), which is created when the first type of oxygen vacancy is further reduced by CO. This second type of site is not as readily reoxidised as the first type and a higher temperature (about 250°C) is needed in order to reoxidise it. This site is thus referred to as an "irreversibly reduced site." At 80°C the rate of reoxidation of the first type of site is higher leading to a lower surface concentration of these sites. This means that the rate of formation of the second type of site from the first type of site will be lower at this temperature explaining the lower rate of deactivation at 80°C. However, if sites of the second type are formed during the reaction at 80°C they will not be reoxidised but the temperature has to be increased to 250°C in order to reoxidise these sites. Cobalt Co^{3+} ions are active for CO oxidation but during the reaction these are reduced to a lower oxidation state resulting in a slow decrease in the number of these ions. The reduced cobalt ions cannot be reoxidised to the active state at ambient temperature and the activity is lost. A similar type of deactivation mechanism has been proposed for the reaction between CO and NO over CuO/ZrO_2 at 250°C (42). In that catalytic cycle Cu^{2+} was reduced to Cu^{+} and then reoxidised to Cu^{2+}. Deactivation occurred when Cu^{+} was reduced by CO to Cu^{0}. Deactivation by reduction of Cu^{2+} has also been observed for CuO/CeO_2, which is active for CO oxidation at 70°C (43). However, as far as we know, experimental observations supporting

this deactivation mechanism have not been reported for room temperature CO oxidation over Co_3O_4. The deactivation mechanism explains why regeneration in O_2 is more efficient than regeneration in Ar alone. During regeneration at 250–350°C in O_2 the deactivated (reduced) cobalt ions are reoxidised to the active state, which could also be observed with XRD and XANES. The regeneration temperature agrees with the temperature region for oxidation of cobalt oxide previously seen with TPO (24). The positive effect of regenerating in 100% Ar seen at a temperature of approximately 350°C is probably explained by bulk oxygen in Co_3O_4 becoming mobile at this temperature. Bulk oxygen can thus diffuse to the surface and fill the oxygen vacancies creating the active Co_3O_4 phase. This mechanism is also consistent with previous studies which have shown that a prereduced catalyst is less active than a preoxidised catalyst (15): prereduction of the catalyst creates more inactive reduced cobalt ions, i.e., having the same effect as deactivating the catalyst. However, this mechanism is not consistent with the XPS measurements where no reduction could be seen during the reaction, not even after exposure to 4% CO. One explanation could be that the number of active sites is small and thus the change is too small to be observed with XPS.

A third explanation for the deactivation of Co_3O_4 during CO oxidation could be that the coordination of the surface cobalt ions is changed but there is no change in oxidation state. The valency and coordination of the surface cobalt ions have been subject to investigation by several authors. Busca *et al.* (32) found that Co_3O_4 after calcination exposed only Co^{3+} sites. These sites were readily reduced by CO at room temperature, producing Co^{2+}. Shirai *et al.* (44) found that Co_3O_4 grown on α-Al_2O_3 (0001) after oxidation at 600°C exposed coordinatively unsaturated oxygen atoms bridging Co^{3+} ions. Omata *et al.* (45) studied the CO and H_2 oxidation over Co_3O_4. By successively substituting the Co^{2+} and Co^{3+} ions in Co_3O_4 with less active Zn^{2+} and Al^{3+} ions respectively they concluded that octahedrally coordinated Co^{3+} ions in the surface are the active site and that tetrahedrally coordinated Co^{2+} is less active. Using a similar ion substitution technique Jacobs *et al.* (46) drew the conclusion that octahedrally coordinated Co^{3+} ions in the surface are active whereas no Co^{2+} ions existed at the surface. We thus suggest that the active site in our mechanism, where CO can adsorb and react at low temperature, is an octahedrally coordinated surface Co^{3+} ion. Yao and Shelef (47) reported that CO chemisorbed on octahedrally coordinated cobalt sites independent of the oxidation state (Co^{2+} and Co^{3+}), while tetrahedrally coordinated cobalt sites were inactive for CO adsorption. In Co_3O_4, the Co^{3+} ions are originally in the octahedral positions and Co^{2+} in tetrahedral positions. As discussed above, it has been shown that octahedrally coordinated Co^{3+} is the ion, which is exposed at the surface of Co_3O_4. If during the CO oxidation reaction a surface reconstruction occurs where active octahedrally coordinated Co^{3+} ions are transformed to tetrahedrally coordinated cobalt ions, the catalyst would lose activity, such as has been observed experimentally. Since no change in oxidation state of the cobalt ions occurs, this process would not be possible to detect with XPS.

CONCLUSIONS

Co_3O_4 deactivated slowly during steady-state CO oxidation at room temperature. The rate of deactivation increased with increasing gas-phase CO or CO_2 concentration but the deactivation could be made less severe by increasing the gas-phase O_2 concentration or increasing the reaction temperature. Neither the formation of surface carbonates, surface carbonyls, nor C_{surf} could explain the slow deactivation of the cobalt oxide. Further, an irreversible reduction mechanism is not supported by XPS data. Instead we suggest that the decrease in activity is due to a surface reconstruction of the cobalt oxide making the cobalt ions inactive for CO adsorption. The deactivated catalyst could be regenerated by oxidising it at 250°C thus re-creating the active Co_3O_4 surface state.

ACKNOWLEDGMENTS

The Competence Centre for Catalysis is financially supported by the Swedish National Energy Administration and member companies: AB Volvo, Johnson Matthey-CSD, Saab Automobile AB, Perstorp AB, MTC AB, Akzo Nobel, and the Swedish Space Corporation. The European Synchrotron Radiation Facility is thanked for granting the XANES beam time, and Dr. Sakura Pascarelli at beamline ID24 is gratefully thanked for her assistance.

REFERENCES

1. Shelef, M., and McCabe, R. W., *Catal. Today* **62**, 35 (2000).
2. Lenaers, G., *Sci. Total Environ.* **189/190**, 139 (1996).
3. Rijkeboer, R. C., *Catal. Today* **11**, 141 (1991).
4. Lafyatis, D. S., Ansell, G. P., Bennett, S. C., Frost, J. C., Millington, P. J., Rajaram, R. R., Walker, A. P., and Ballinger, T. H., *Appl. Catal. B* **18**, 123 (1998).
5. Umehara, K., Tateishi, T., Nishimura, H., and Misumi, M., *JSAE Rev.* **18**, 67 (1997).
6. Chi-Sheng Wu, J., Lin, Z.-A., Tsai, F.-M., and Pan, J.-W., *Catal. Today* **63**, 419 (2000).
7. Drewsen, A., Licentiate thesis, Chalmers University of Technology, Gothenburg, Sweden, 1999.
8. Erkfeldt, S., Jobson, E., and Larsson, M., *Top. Catal.* **16/17**, 127 (2001).
9. Gardner, S. D., Hoflund, G. B., Upchurch, B. T., Schryer, D. S., Kielin, E. J., and Schryer, J., *J. Catal.* **129**, 114 (1991).
10. Sato, H., and Tsuchida, E., *Trans. IEICE* **E73(9)**, 1525 (1990).
11. Watanabe, N., Yamashita, H., Miyadera, H., and Tominaga, S., *Appl. Catal. B* **8**, 405 (1996).
12. Haruta, M., Tsubota, S., Kobayashi, T., Kageyama, H., Genet, M. J., and Delmon, B., *J. Catal.* **144**, 175 (1993).
13. Yamaura, H., Moriya, K., Miura, N., and Yamazoe, N., *Sens. and Actuators, B* **65**, 39 (2000).

14. Funazaki, N., Hemmi, A., Ito, S., Asano, Y., Yamashita, S., Kobayashi, T., and Haruta, M., *Sens. Actuators B* **13–14**, 536 (1993).
15. Thormählen, P., Skoglundh, M., Fridell, E., and Andersson, B., *J. Catal.* **188**, 300 (1999).
16. Yu Yao, Y.-F., *J. Catal.* **33**, 108 (1974).
17. Cunningham, D. A. H., Kobayashi, T., Kamijo, N., and Haruta, M., *Catal. Lett.* **25**, 257 (1994).
18. Simonot, L., Garin, F., and Maire, G., *Appl. Catal. B* **11**, 167 (1997).
19. Simonot, L., Garin, F., and Maire, G., *Stud. Surf. Sci. Catal.* **96**, 203 (1995).
20. Meng, M., Lin, P., and Fu, Y., *Catal. Lett.* **48**, 213 (1997).
21. Mergler, Y. J., Hoebink, J., and Nieuwenhuys, B. E., *J. Catal.* **167**, 305 (1997).
22. Mergler, Y. J., van Aalst, A., van Delft, J., and Nieuwenhuys, B. E., *Stud. Surf. Sci. Catal.* **96**, 163 (1995).
23. Mergler, Y. J., van Aalst, A., van Delft, J., and Nieuwenhuys, B. E., *Appl. Catal. B* **10**, 245 (1996).
24. Jansson, J., *J. Catal.* **194**, 55 (2000).
25. Jansson, J., Skoglundh, M., Fridell, E., and Thormählen, P., *Top. Catal.* **16/17**, 385 (2001).
26. Sanchez del Rio, M., and Dejus, R. J., *in* "XOP: Recent Developments," Vol. 2448, p. 340. SPIE—Int. Soc. Opt. Eng., Bellingham, WA, 1998.
27. Takita, Y., Tashiro, T., Saito, Y., and Hori, F., *J. Catal.* **97**, 25 (1986).
28. Davydov, A. A., *in* "Infrared Spectroscopy of Adsorbed Species on the Surface of Transition Metal Oxides" (C. H. Rochester, Ed.), p. 6–62. Wiley, New York, 1990.
29. Al-Mashta, F., Sheppard, N., Lorenzelli, V., and Busca, G., *J. Chem. Soc., Faraday Trans. 1* **78**(3), 979 (1982).
30. Todorova, S., Zhelyazkov, V., and Kadinov, G., *React. Kinet. Catal. Lett.* **57**(1), 105 (1996).
31. Mergler, Y. J., van Aalst, A., van Delft, J., and Nieuwenhuys, B. E., *J. Catal.* **161**, 310 (1996).
32. Busca, G., Guidetti, R., and Lorenzelli, V., *J. Chem. Soc., Faraday Trans.* **86**(6), 989 (1990).
33. Schönnenbeck, M., Cappus, D., Klinkmann, J., Freund, H.-J., Petterson, L. G. M., and Bagus, P. S., *Surf. Sci.* **347**, 337 (1996).
34. Christoskova, St. G., Stoyanova, M., Georgieva, M., and Mehandjiev, D., *Mater. Chem. Phys.* **60**(1), 39 (1999).
35. Arnoldy, P., and Moulijn, J. A., *J. Catal.* **93**, 38 (1985).
36. van't Blik, H. F. J., and Prins, R., *J. Catal.* **97**, 188 (1986).
37. Wang, W.-J., and Chen, Y.-W., *Appl. Catal.* **77**, 223 (1991).
38. Shen, Z. X., Allen, J. W., Lindberg, P. A. P., Dessau, D. S., Wells, B. O., Borg, A., Ellis, W., Kang, J. S., Oh, S. J., Lindau, I., and Spicer, W. E., *Phys. Rev. B* **42**, 1817 (1990).
39. Moulder, J. F., Stickle, W. F., Sobol, P. E., and Bomben, K. D., "Handbook of X-Ray Photoelectron Spectroscopy," Perkin Elmer Corporation Wellesley, MA, 1992.
40. Oku, M., and Sato, Y., *Appl. Surf. Sci.* **55**, 37 (1992).
41. Bridge, M. E., and Lambert, R. M., *Surf. Sci.* **82**, 413 (1979).
42. Okamoto, Y., Kubota, T., Gotoh, H., Ohto, Y., Aritani, H., Tanaka, T., and Yoshida, S., *Faraday Trans*. **94**, 3743 (1998).
43. Harrison, P. G., Ball, I. K., Azelee, W., Daniell, W., and Goldfarb, D., *Chem. Mater.* **12**, 3715 (2000).
44. Shirai, M., Inoue, T., Onishi, H., Asakura, K., and Iwasawa, Y., *J. Catal.* **145**, 159 (1994).
45. Omata, K., Takada, T., Kasahara, S., and Yamada, M., *Appl. Catal. A* **146**, 255 (1996).
46. Jacobs, J.-P., Maltha, A., Reintjes, J. G. H., Drimal, J., Ponec, V., and Brongersma, H. H., *J. Catal.* **147**, 294 (1994).
47. Yao, H. C., and Shelef, M., *J. Phys. Chem.* **78**(24), 2490 (1974).